Sensors and Materials, Vol. 17, No. 6 (2005) 343–353
MYU Tokyo

S & M 0612

Introduction of InP-Based Light Emitter into GaAs-Based 3D Photonic Crystal by Improved Wafer Bonding of Dissimilar Materials

Masahiro Imada*, Shinpei Ogawa, Susumu Yoshimoto, and Susumu Noda**

Department of Electronic Science and Engineering, Kyoto University, Kyoto 615-8510, Japan

(Received January 10, 2005; accepted June 22, 2005)

Key words: optical material, photonic crystal, thermal stress, wafer bonding

We developed improved wafer-bonding techniques for dissimilar materials in order to introduce an InP-based light emitter into a GaAs-based three-dimensional (3D) photonic crystal (PC). Observation of the GaAs/InGaAsP-bonding interface by scanning acoustic microscopy revealed that debonding occurred at approximately 300°C due to the differing thermal expansion coefficients of GaAs and InP. We calculated thermal stress using a 2D finite-element method and found that it could be reduced by thinning the InP substrate. These results were used to successfully develop a 3D PC incorporating a multiple quantum-well light-emitting structure and artificial defects. Photoluminescence measurements revealed that spontaneous emission within the PC region was reduced due to the complete photonic band gap, while strong emission due to the defect state was observed only within the defect region. These results are important steps towards the realization of novel light-sources, such as zero-threshold lasers, using 3D PCs.

Photonic crystals (PCs), which are artificial structures in which periodic refractive-index variation is created, have recently attracted much interest.[1–3] PCs exhibit a photonic band gap (PBG) region in which the propagation and emission of electromagnetic waves is prohibited for all wave vectors within the PBG. With the aid of artificially introduced defects and/or light emitters, such crystals are becoming powerful tools for the complete control of photons. Although remarkable progress has been made with two-dimensional (2D) PCs,[4–17] there is increasing interest in 3D PCs[2,3,18–30] because they exhibit a PBG in all three spatial dimensions so that complete control of light is expected. For example, suppression and/or enhancement of spontaneous emission have been investigated from the

*Corresponding author, e-mail address: imada@kuee.kyoto-u.ac.jp
**Corresponding author, e-mail address: snoda@kuee.kyoto-u.ac.jp

initial stages in PC research.[1] In order to realize such physically interesting phenomena, several requirements need to be satisfied. First, the construction of 3D PCs with a complete PBG in the optical communications wavelength region is necessary. Secondly, the introduction of both an efficient light-emitting layer and artificial defects at arbitrary positions within the crystal are also important for the development of applications. Third and finally, the crystal needs to be electrically conducting, which is crucial for the realization of optoelectronic devices. There are various methods for fabricating 3D PCs, such as the self-assembled growth of colloidal crystals,[22,23] an Si-based crystal utilizing layer-by-layer growth,[24,25] a 2D periodic structure stacked by micromanipulation under scanning electron microscopy (SEM) observation[26] and laser-writing techniques.[27–29] However, it is difficult for these methods to simultaneously satisfy the three key requirements listed above. In 1994, we proposed an original fabrication method based on the precise alignment and wafer fusion of 2D periodic structures constructed by electron-beam (EB) lithography, followed by reactive ion etching.[2] In 2000, we developed 3D PCs with a complete PBG in the 1.55 μm wave length region,[3] which satisfied the first of the requirements listed above. The requirement that the introduction of artificial defects can also be satisfied as the development method is based upon the stacking of 2D structures so that an artificial defect can be arbitrarily introduced by simply changing the pattern that is drawn by EB lithography for a specific layer. The final requirement has already been successfully implemented using this approach, as demonstrated by the operation of a room-temperature current-injected 2D PC laser constructed by the wafer-fusion technique.[31–34]

The remaining issue is the introduction of a light-emitting material, which might be satisfied by the incorporation of an InGaAsP multiple quantum well (MQW) layer into the GaAs-based 3D PC. However, wafer fusion of dissimilar materials, such as GaAs and InP, is difficult due to the difference in the thermal expansion coefficients of these materials. To overcome this problem, we have successfully developed an improved technique for the wafer fusion of dissimilar materials,[35] which has recently led to the demonstration of controlled light emission in a 3D PC.[30] In the current paper, we describe the introduction of an InP-based light-emitter into a GaAs-based 3D PC using the improved wafer-fusion technique and present a basic optical characterization of this light-emitting device.

The wafer-fusion technique, which was initially applied to the integration of Si-on-Si and Si-on-insulator (SOI),[36,37] has been extensively studied for the integration of different materials. For example, in the 1990s, the technique was applied to the integration of III-V materials.[38] InP- and GaAs-based structures, such as lasers on Si,[39–43] InP-based structures on GaAs[44–51] and several others,[52–57] have also been reported. The most important advantage wafer-fusion offers is that it enables the construction of highly lattice-mismatched heterostructures, without the formation of threading dislocations, whilst retaining an electrically conductive interface. Although there have been many previous reports on the wafer fusion of dissimilar materials, there have been few studies of wafer fusion with precise alignment. In order to realize 3D PCs incorporating light-emitting layers, wafer-fusion techniques for dissimilar materials must be developed with extremely precise layer alignment.

Figure 1(a) shows a schematic of the structure developed in the present work, which has a stacked stripe or 'woodpile' structure.[18] A light-emitting layer with a similar stripe geometry is sandwiched between GaAs PC layers, without disturbing the periodicity of the crystal, so that the structure has five layers in total. The period, width and thickness of the stripes within each layer (including the light-emitting layer) are 0.7, 0.2 and 0.2 μm, respectively. The light-emitting layer incorporates a three-period InGaAsP MQW structure grown by metallorganic vapor-phase epitaxy (MOVPE). The MQW has been fabricated to have a peak emission wavelength of 1.5 μm, which falls within the wavelength

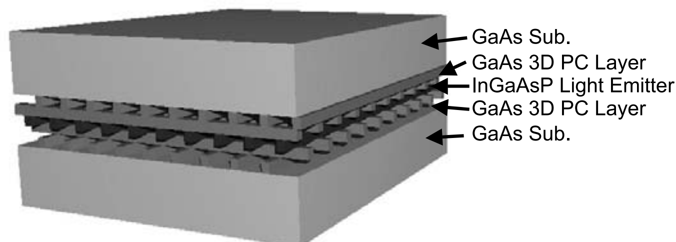

(a)

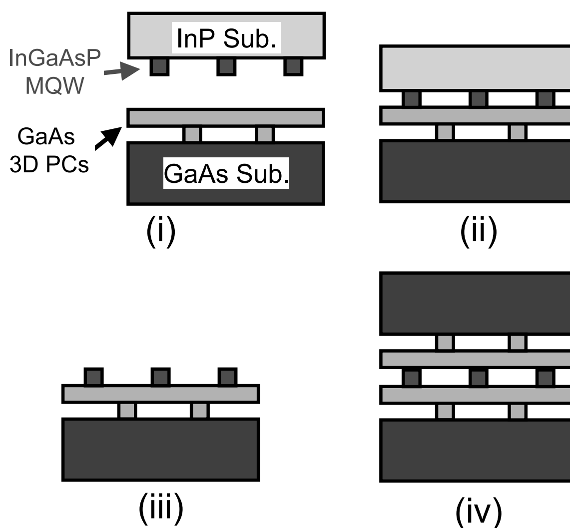

(b)

Fig. 1. Schematic of (a) a five-layer stacked 3D PC incorporating an InGaAsP MQW and (b) the procedure used to fabricate the 3D PC containing a light-emitting region. (i) The 3D PC is prepared on a GaAs substrate, while the light-emitting structure is prepared on an InP substrate. Both structures are aligned precisely. (ii) The wafers are brought into contact and hydrogen bonded. (iii) The sample is heated in a hydrogen atmosphere and fused at temperatures of up to 525°C. The InP substrate is then removed by wet etching. (iv) Steps (i)–(iii) are repeated in order to a construct a multilayer 3D PC device incorporating a MQW light-emitting region.

range of the complete PBG of the crystal. Figure 1(b) shows the fabrication process before improvements were made. Figures 1(b(i)) and 1(b(ii)) schematically depict the 3D PC on a GaAs substrate and the light-emitting layer on its InP substrate before and after fusing. The layers are pretreated with a buffered HF solution (50% HF : 40% NH_4F = 1:6) to remove a native oxide layer, followed by treatment with an organic alkali to terminate the surfaces with hydroxyl groups. The two layers are then precisely aligned so that weak hydrogen bonding occurs between the hydroxyl groups on each surface. This enables safe handling of the contacted wafer without disturbing the alignment. The layers are then heated to above 500°C in a hydrogen atmosphere and fused. Figure 1(b(iii)) depicts the removal of the InP substrate, which is achieved via a mechanical and chemical (35% HCl : H_2O = 1:4) thinning process, resulting in a structure with the light-emitting layer integrated on top of the GaAs-based 3D PC. We prepared a second 3D PC and fused this on top of the light-emitting layer (depicted in Fig. 1(b(iv))) by repeating processes Fig. 1(b(i)) and 1(b(ii)), resulting in the structure shown in Fig. 1(a). The important point in this process is that the two wafers are precisely aligned at room temperature, via hydrogen bonding, before the heating process strongly bonds the layers together in these exact positions without disturbing the alignment.

To investigate the influence of thermal stress on the fused interface, we utilized scanning acoustic microscopy (SAM).[58] A scanning acoustic microscope utilizes the propagation and reflection of acoustic waves at interfaces where a change in acoustic impedance occurs. The acoustic impedance of a material is defined by multiplying the density by the velocity of acoustic waves of the material. Because the acoustic impedance difference between a semiconductor (GaAs or InP) and air is large, it is possible to nondestructively detect debonding areas where air exists between the wafers. The acoustic wave frequency used in this work was 110 MHz and the spatial resolution was ~10 μm. Figure 2(a) shows SAM images of the wafers bonded by room-temperature hydrogen bonding before heating.[35] The five white areas at the center of the image are indicative of the 3D PC, which corresponds to the structure shown in Fig. 1(a). The other areas have different stripe widths and pitches, mainly for discharging gases during heating and alignment, which reflect the contrast of the SAM image. There are no areas of high reflection, which suggests that at room temperature, uniform bonding occurred across the whole surface. Note that the white area around the sample is not indicative of debonding; this results from an overhang due to a size difference between the upper and lower wafers. Figure 2(b) shows a SAM image of the same sample after being heated at 525°C for 2 h in a hydrogen atmosphere under the pressure of 0.3 kgf/cm^2 to the wafers (these are conventional wafer-fusion conditions for GaAs).[35] It is clear that the white region corresponding to an area of high reflectance spreads across most of the wafer, suggesting that debonding occurs during heating. Without SAM observation, the two wafers appear to be strongly bonded together after heating; however, this is shown not to be the case when the two wafers separate as the wafer is thinned. This phenomenon is not observed when two wafers of the same material, such as GaAs, are bonded. These results indicate that thermal stress due to the difference in thermal expansion coefficients makes the bonding interface break up during the heating procedure. This can be explained by an increase in strain energy due to thermal stress as the temperature is increased past the point where it exceeds the surface

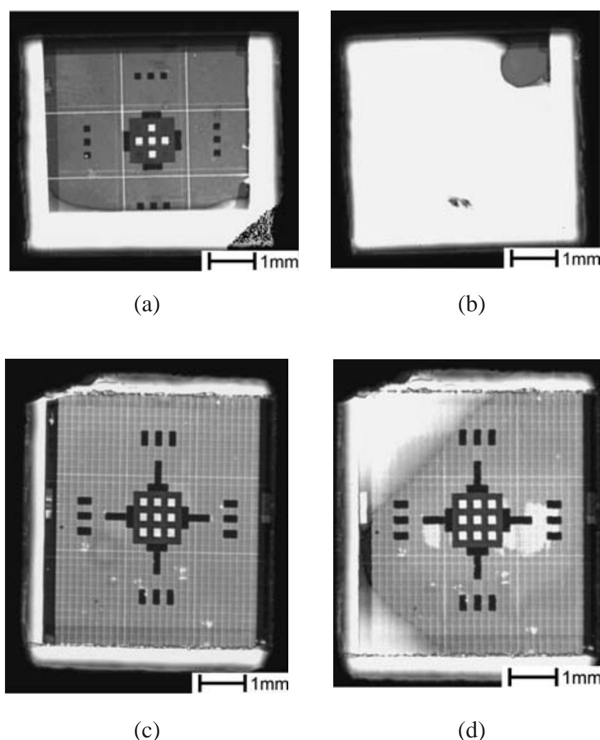

Fig. 2. SAM images of the bonding interface. Five white regions at the center of the image are indicative of a 3D PC. The other areas have different stripe pitches, which are mainly used for emitting gas, and for alignment that reflect the contrast of the SAM image. (a) Image of the interface between the GaAs-based PC and the InP-based light emitter hydrogen-bonded at room temperature. (b) Image of the interface after heating at 525°C. (c) SAM image of the GaAs-based PC and the InP-based light emitter heated at 220°C. (d) SAM image of the GaAs-based PC and the InP-based light emitter heated at 300°C.

energy of the bonding interface. There are two possible methods for reducing thermal stresses. First, the fusing temperature could be reduced. However, we have found that the surface energy of a sample heated at low temperatures is not sufficient for strong bonding. When the InP substrate is completely removed, the PC structure breaks in the region where the bonding is weakest. Secondly, an alternative method involves reducing the wafer thickness before heating, as in Wada and Kamijoh's work.[52] However, this makes wafer handling and precise alignment difficult. To satisfy the requirement for high bonding strength without making wafer handling and precise alignment difficult, we investigated a multistep wafer-fusion technique that utilizes a cycle of heating and thinning.

Initially, it was important to investigate the critical temperature at which debonding occurs. Figure 2(c) shows a SAM image after heating at 220°C for 60 h under a pressure of 8 kgf/cm^2, while Fig. 2(d) is a SAM image of the same sample after heating at 300°C for 60 h under the same pressure. Clearly, no debonding area is observed in Fig. 2(c), while Fig. 2(d)

shows debonding initiated at the wafer edge. This indicates that the thermal stresses exceed the surface energy of the bonding interface so that debonding initiates at about 300°C. In order to analyze this in more detail, a 2D finite-element method (FEM) was used to calculate the strain energy caused by thermal stress. Figure 3(a) shows the dependence of strain energy on the temperature.(35) A comparison of Fig. 2(d) with Fig. 3(a) suggests that the surface energy of the sample heated to 220°C can be estimated to lie between 1,000 and 2,000 mJ/m^2. This value is in good agreement with the surface energy of ~1,500 mJ/m^2 reported for hydrogen bonding between hydroxyl groups in this temperature range.(59) This indicates that the strain energy during heating should be kept below 2,000 mJ/m^2 in order to prevent debonding. Figure 3(b) shows the calculated dependence of strain energy on InP wafer thickness for heating at temperatures of 300°C and 525°C.(35) It is clear that the strain energy can be reduced below the critical energy by thinning the InP substrate to below 20 µm, even when the sample is heated to 525°C. At 300°C, the same effect can be achieved when the InP substrate is thinned to about 150 µm. The calculated results have been confirmed experimentally.(35) These results indicate that the structure shown in Fig. 1(a) can be constructed by a three-step wafer-fusion process. First, the wafers are bonded by low-temperature (220°C) heating after precise alignment. Secondly, the InP substrate is thinned below 150 µm to reduce thermal stresses before being bonded at 300°C to increase the bond energy. Third and finally, the InP substrate is thinned below ~1 µm by selective wet etching to further reduce thermal stresses before the sample is heated to ~525°C to fuse the wafers firmly.

We utilized this three-step wafer-fusion technique to develop a 3D PC incorporating a light-emitting layer and artificial defects, as shown in Fig. 4. Two artificial defects of different sizes, labeled A and B, were formed in the light-emitting layer. Figure 4 includes a schematic of the regions of the PC around defects A and B, with the insets showing SEM images of these regions observed from an oblique direction after stacking the lower GaAs 3D PC layers. Defects A and B have areas of 1.6×3.0 and 2.3×3.6 µm^2, respectively. In order to evaluate the effect of the PBG and the defects on the spontaneous-emission profile of the MQW, we also prepared a reference area on the same wafer where an identical light-

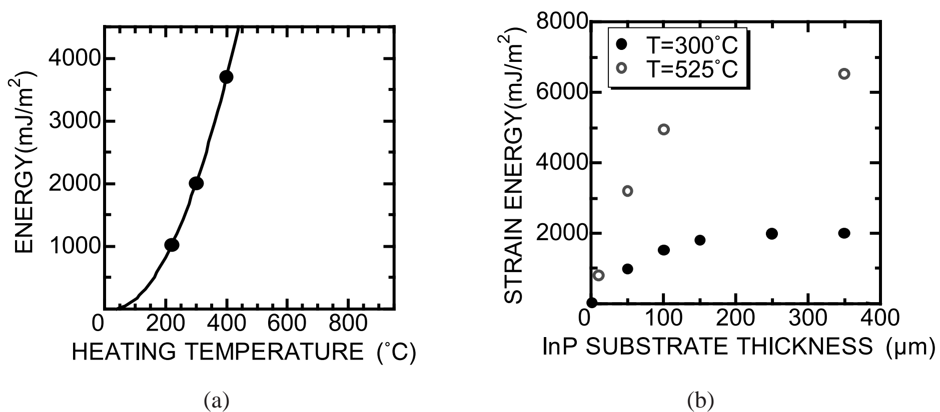

(a) (b)

Fig. 3. (a) Calculated thermal strain energy as a function of annealing temperature. (b) Calculated results for thermal strain energy as a function of wafer thickness for heating at both 525 and 300°C.

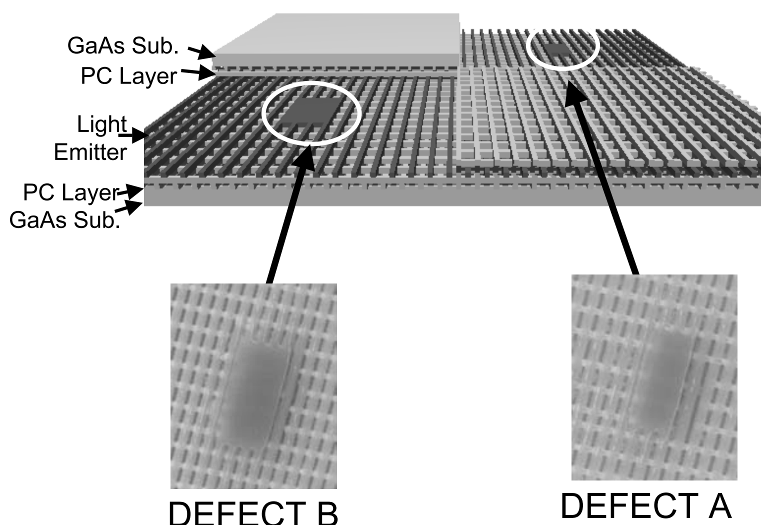

Fig. 4. Schematic of the five-layer stacked 3D PC incorporating the InGaAsP MQW light emitter and artificial defects. The insets show SEM images, observed from an oblique direction, of defects A and B after being stacked on top of the two-layer GaAs 3D PC.

emitting layer with the same stripe geometry was sandwiched between unpatterned (flat) GaAs layers. A comparison of the emission spectra from these two regions allows for an evaluation of the effects of the PBG. Our previous report(3) has already demonstrated that the structure has a complete PBG in the 1.3 to 1.55 µm wavelength region.

We detected and compared the photoluminescence (PL) spectra from four regions on the structure: (i) a PC region away from defects (ii) the region at defect A (iii) the region at defect B and (iv) a reference region without PC. The PL spectra were measured at room temperature by a micro-PL method. The sample was excited by a continuous wave Ti-Sapphire laser at a wavelength of 900 nm, which corresponds to a pass band of the PC. PL emission was detected normally from a circular region of diameter ~2 µm. Figure 5 shows the PL intensity from regions (i) to (iii), normalized by the PL intensity from region (iv). Clearly, the normalized PL intensity of the PC region is below 1 within the PBG wavelength region. A stripe pattern was also formed in the reference region in order to confirm that the weakened emission is not due to dry-etching damage or a surface-recombination effect in the MQW. We confirmed that suppression of spontaneous emission is only observed in the wavelength region where a complete PBG exists.(21) These results indicate that the PL reduction in region (i) is due to the suppression of spontaneous emission as a result of the PBG effect. In contrast, the PC regions containing defects A and B exhibit a normalized PL intensity which differs from region (i). PL from region (ii) exhibited a strong peak at 1.42 µm, while emission was suppressed at all other wavelengths. An emission peak was observed in region (iii) at 1.48 µm. Figure 6 shows PL intensity mapping results from regions (ii) and (iii) for two different detection wavelengths. When the wavelength corresponded to the peak emission wavelength from defect A, strong emission was only observed from defect A, while the emission intensity from defect B and

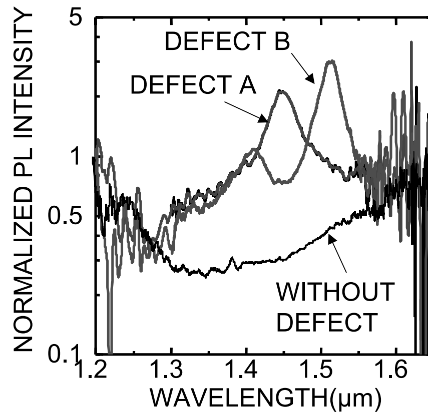

Fig. 5. Normalized PL intensity of the PC area without defects (black line), and the PC areas with defects A (blue line) and B (red line).

the PC regions without defects was small, as shown in Fig. 6(a). Conversely, when the detection wavelength corresponded to the peak emission wavelength from defect B, emission from defect A became weak, while strong emission was only observed from defect B, as shown in Fig. 6(b). Here, we must note that the light-emitting layer is formed all over the measured area, as mentioned above. These results suggest that strong emission is only possible from the defect areas at the wavelength within the PBG at which the defect state exists. The insets of Fig. 6 show a magnification of the PL mapping around the defect areas. The strongly emitting regions are several micrometers wide, which is comparable to the resolution limit of the micro-PL equipment. These results indicate that the defects act as 3D PC defect cavities. In this structure, the defects are relatively large, being several micrometers in size, while there are only five stacked layers. Recently, we have developed a nine-layer stacked 3D PC structure with a light-emitting layer and much smaller artificial defects. In this structure, we observed an even stronger reduction in emission intensity within the PC region without defects and even sharper PL peaks in the defect areas.(30) These results constitute important steps towards the realization of novel light sources.

In summary, we investigated the wafer-fusion conditions for different materials in order to develop a 3D PC incorporating a light-emitting layer. We observed the bonding interface by SAM and found that debonding occurred at temperatures above 300°C due to the difference in the thermal expansion coefficients of the materials. We calculated the strain energy caused by thermal stress and showed that this could be kept below the wafer surface energy by thinning the substrate, even at elevated temperatures. We also experimentally demonstrated thermal stress reduction, which led to the successful development of a 3D PC incorporating a light-emitting layer and artificial defects. PL measurement demonstrated that spontaneous emission from the PC region was reduced due to the complete PBG effect, while strong emission was only observed from defects, due to the creation of a defect state within the PBG. These results are important for the development of wafer fusion for other materials, such as a GaAs and Si or InP and Si, and represent important steps towards the realization of novel light sources, such as zero-threshold lasers.

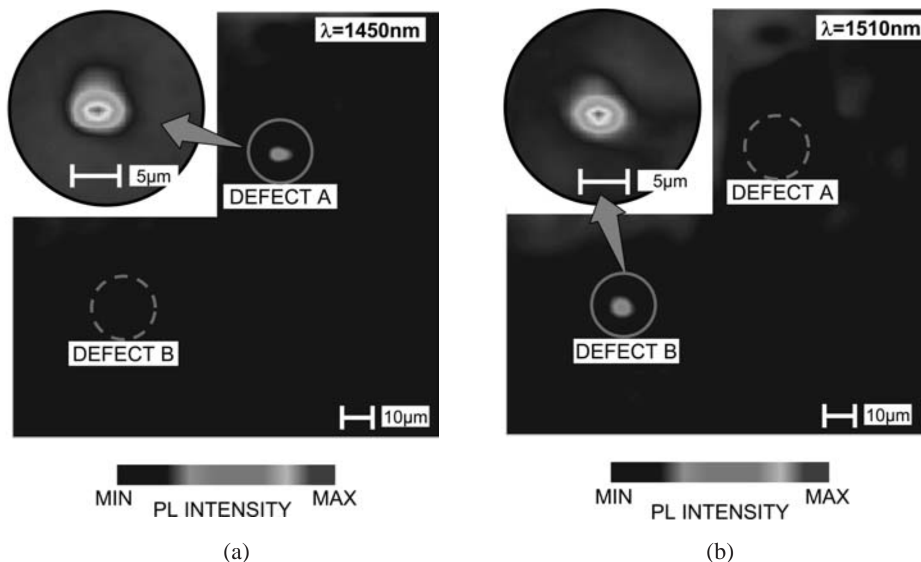

Fig. 6. PL intensity mapping, measured by micro-PL (spatial resolution: ~2 μm) at different detection wavelengths. (a) PL at 1,450 nm corresponds to the peak emission wavelength of defect A. The inset shows a magnified PL map around defect A. (b) PL at 1,510 nm corresponds to the peak emission wavelength of defect B. The inset shows a magnified PL map at defect B.

Acknowledgements

The authors would like to thank Mr. M. Yokoyama for valuable discussions. This work was partly supported by the Core Research for Evolutional Science and Technology Program from the Japan Science and Technology Agency, by a Grant-in-Aid for Scientific Research of Priority Areas from the Ministry of Education, Culture, Sports, Science and Technology of Japan, and by the Venture Business Laboratory of Kyoto University, Japan.

References

1 E. Yablonovitch: Phys. Rev. Lett. **58** (1987) 2059.
2 S. Noda, N. Yamamoto and A. Sasaki: Jpn. J. Appl. Phys. **35** (1996) L909.
3 S. Noda, K. Tomoda, N. Yamamoto and A. Chutinan: Science **289** (2000) 604.
4 O. Painter, R. K. Lee, A. Scherer, A. Yariv, J. D. O'Brien, P. D. Dapkus and I. Kim: Science **284** (1999) 1819.
5 H. G. Park, S. H. Kim, S. H. Kwon, Y. G. Ju, J. K. Yang, J. H. Baek, S. B. Kim and Y. H. Lee: Science **305** (2004) 1444.
6 S. Noda, A. Chutinan and M. Imada: Nature **407** (2000) 608.
7 B. S. Song, S. Noda and T. Asano: Science **300** (2003) 1537.
8 Y. Akahane, T. Asano, B. S. Song and S. Noda: Nature **425** (2003) 944.
9 T. F. Krauss, R. M. DelaRue and S. Brand: Nature **383** (1996) 699.

10 H. Benisty, C. Weisbuch, D. Labilloy, M. Rattier, C. J. M. Smith, T. F. Krauss, R. M. DelaRue, R. Houdre, U. Oesterle, C. Jouanin and D. Cassagne: IEEE/OSA J. Lightwave Technol. **17** (1999) 2063.
11 T. Baba, N. Fukaya and J. Yonekura: Electron. Lett. **35** (1999) 654.
12 M. Notomi, A. Shinya, K. Yamada, J. Takahashi, C. Takahashi and I. Yokohama: IEEE J. Quantum Electron. **38** (2002) 736.
13 S. J. McNab, N. Moll and Y. A. Vlasov: Opt. Express **11** (2003) 2927.
14 D. Mori and T. Baba: Appl. Phys. Lett. **85** (2004) 1101.
15 T. D. Happ, M. Kamp and A. Forchel: Opt. Lett. **26** (2001) 1102.
16 P. Kramper, M. Agio, C. M. Soukoulis, A. Birner, F. Müller, R. B. Wehrspohn, U. Gösele and V. Sandoghdar: Phys. Rev. Lett. **92** (2004) 113903.
17 E. Chow, S. Y. Lin, S. G. Johnson, P. R. Villeneuve, J. D. Joannopoulos, J. R. Wendt, G. A. Vawter, W. Zubrzycki, H. Hou and A. Alleman: Nature **407** (2000) 983.
18 K. M. Ho, C. T. Chan, C. M. Soukoulis, R. Biswas and M. Sigalas: Solid State Commun. **89** (1994) 413.
19 I. Bulu, H. Caglayan and E. Ozbay: Phys. Rev. B **67** (2003) 205103.
20 M. Megens, J. Wijnhoven, A. Lagendijk and W. L. Vos: Phys. Rev. A **59** (1999) 4727.
21 S. Noda, M. Imada, M. Okano, S. Ogawa, M. Mochizuki and A. Chutinan: IEEE J. Quantum Electron. **38** (2002) 726.
22 H. Míguez, C. Lóez, F. Meseguer, A. Blanco, L. Vázquez, R. Mayoral, M. Ocaña, V. Fornés and A. Mifsud: Appl. Phys. Lett. **71** (1997) 1148.
23 A. Blanco, E. Chomski, S. Grabtchak, M. Ibisate, S. John, S.W. Leonard, C. Lopez, F. Meseguer, H. Miguez, J. P. Mondia, G. A. Ozin, O. Toader and H. M. van Driel: Nature **405** (2000) 437.
24 J. G. Fleming and S. Y. Lin: Opt. Lett. **24** (1999) 49.
25 M. Qi, E. Lidorikis, P. T. Rakich, S. G. Johnson, J. D. Joannopoulos, E. P. Ippen and H. I. Smith: Nature **429** (2004) 538.
26 K. Aoki, H. T. Miyazaki, H. Hirayama, K. Inoshita, T. Baba, K. Sakoda, N. Shinya and Y. Aoyagi: Nature Materials **2** (2003) 117.
27 M. Campbell, D. N. Sharp, M. T. Harrison, R. G. Denning and A. J. Turberfield: Nature **404** (2000) 53.
28 V. Mizeikis, K. K. Seet, S. Juodkazis and H. Misawa: Opt. Lett. **29** (2004) 2061.
29 M. Deubel, G.V. Freymann, M. Wegener, S. Pereira, K. Busch and C. M. Soukoulis: Nature Materials **3** (2004) 444.
30 S. Ogawa, M. Imada, S. Yoshimoto, M. Okano and S. Noda: Science **305** (2004) 227.
31 M. Imada, S. Noda, A. Chutinan, T. Tokuda, M. Murata and G. Sasaki: Appl. Phys. Lett. **75** (1999) 316.
32 S. Noda, M. Yokoyama, M. Imada, A. Chutinan and M. Mochizuki: Science **293** (2001) 1123.
33 D. Ohnishi, K. Sakai, M. Imada and S. Noda: Electron. Lett. **39** (2003) 612.
34 D. Ohnishi, T. Okano, M. Imada and S. Noda: Opt. Express **12** (2004) 1562.
35 S. Ogawa, M. Imada and S. Noda: Appl. Phys. Lett. **82** (2003) 3406.
36 J. B. Lasky: Appl. Phys. Lett. **48** (1986) 78.
37 M. Shimbo, K. Furukawa, K. Fukuda and K. Tanzawa: J. Appl. Phys. **60** (1986) 2987.
38 Z. L. Liau and D. E. Mull: Appl. Phys. Lett. **56** (1990) 737.
39 Y. H. Lo, R. Bhat, D. M. Hwang, C. Chua and C.-H. Lin: Appl. Phys. Lett. **62** (1993) 1038.
40 H. Wada and T. Kamijoh: Jpn. J. Appl. Phys. **33** (1994) 4878.
41 K. Mori, K. Tokutome and S. Sugou: Electron. Lett. **31** (1995) 284.
42 F. E. Ejeckam, C. L. Chua, Z. H. Zhu, Y. H. Lo, M. Hong and R. Bhat: Appl. Phys. Lett. **67** (1995) 3936.

43 A. Fontcuberta i Morral, J. M. Zahler, Harry A. Atwater, S. P. Ahrenkiel and M. W. Wanlass: Appl. Phys. Lett. **83** (2003) 5413.
44 Y. H. Lo, R. Bhat, D. M. Hwang, M. A. Koza and T. P. Lee: Appl. Phys. Lett. **58** (1991) 1961.
45 J. J. Dudley, D. I. Babic, R. Mirin, L. Yang, B. I. Miller, R. J. Ram, T. Reynolds, E. L. Hu and J. E. Bowers: Appl. Phys. Lett. **64** (1994) 1463.
46 I.-H. Tan, J. J. Dudley, D. I. Babic, D. A. Cohen, B. D. Yang, E. L. Hu, J. E. Bowers, B. I. Miller, U. Koren and M. G. Young: IEEE Photon. Technol. Lett. **6** (1994) 811.
47 D. I. Babic, J. J. Dudley, K. Streubel, R. P. Mirin, J. E. Bowers, E. L. Hu: Appl. Phys. Lett. **66** (1995) 1030.
48 Y. Okuno, M. Aoki, T. Tsuchiya and K. Uomi: Appl. Phys. Lett. **67** (1995) 810.
49 G. Patriarche, F. Jeannes, J.-L. Oudar and F. Glas: J. Appl. Phys. **82** (1997) 4892.
50 L. Sagalowicz, A. Rudra, E. Kapon, M. Hammar, F. Salomonsson, A. Black, P.-H. Jouneau and T. Wipijewski: J. Appl. Phys. **87** (2000) 4135.
51 F. Shi, S. MacLaren, C. Xu, K. Y. Cheng and K. C. Hsieh: J. Appl. Phys. **93** (2003) 5750.
52 H. Wada and T. Kamijoh: IEEE J. Sel. Topics in Quantum Electron. **3** (1997) 937.
53 F. A. Kish, D. A. DeFevere, D. A. Vanderwater, G. R. Trott, R. J. Weiss and J. S. Major, Jr.: Electron. Lett. **30** (1994) 1790.
54 F. A. Kish, D. A. Vanderwater, M. J. Ludowise, S. G. Hummel and S. J. Rosner: Appl. Phys. Lett. **67** (1995) 2060.
55 R. J. Ram, J. J. Dudley, J. E. Bowers, L. Yang, K. Carey, S. J. Rosner and K. Nauka: J. Appl. Phys. **78** (1995) 422.
56 Y. Okuno, K. Uomi, M. Aoki and T. Tsuchiya: IEEE J. Quantum Electron. **33** (1997) 959.
57 T. Akatsu, A. Plössl, R. Scholz, H. Stenzel and U. Gösele: J. Appl. Phys. **90** (2001) 3856.
58 A. R. Lemons and C. F. Quate: Appl. Phys. Lett. **24** (1974) 163.
59 Q. -Y. Tong, E. Schmidt, U. Gösele and M. Reiche: Appl. Phys. Lett. **64** (1994) 625.